INSTITUTE OF PHYSICS PUBLISHING JOURNAL OF PHYSICS B: ATOMIC, MOLECULAR AND OPTICAL PHYSICS

J. Phys. B: At. Mol. Opt. Phys. **39** (2006) 3519–3528 doi:10.1088/0953-4075/39/17/009

Dissociative and non-dissociative ionization of the N_2 molecule by the impact of 0.75–3.5 MeV He^+

W S Melo[1], A C F Santos[2], M M Sant'Anna[2], G M Sigaud[3] and E C Montenegro[2]

[1] Departamento de Física, Universidade Federal de Juiz de Fora, Juiz de Fora, MG 36036-330, Brazil
[2] Instituto de Física, Universidade Federal do Rio de Janeiro, Rio de Janeiro, RJ, Caixa Postal 68528, 21941-972, Brazil
[3] Departamento de Física, Pontifícia Universidade Católica do Rio de Janeiro, Rio de Janeiro, RJ, Caixa Postal 38031 22452-970, Brazil

E-mail: toni@if.ufrj.br

Received 25 April 2006, in final form 3 July 2006
Published 14 August 2006
Online at stacks.iop.org/JPhysB/39/3519

Abstract

Total projectile electron loss and absolute dissociative and non-dissociative ionization cross sections of the N_2 molecule in coincidence with the final projectile charge states have been measured for the impact of 0.75–3.5 MeV He^+. Comparison is made with proton, He^+ and electron impact data available in the literature for the direct ionization channels. The fragmentation fractions for singly-charged products follow a scaling law indicating that the main dynamical variables behind the fractions are the momentum transfer at intermediate velocities and the energy transfer at high velocities.

1. Introduction

One important feature of the interaction of swift particles with atmospheric gases is the production of molecular fragments and ions which can have a deep influence in changing the inventory of the atmospheric constituents through the gas-phase chemistry that occurs after the fragmentation. Among the atmospheric gases, N_2 is of special importance for being the major atmospheric component of the Earth and of Titan, the Saturn moon.

High energy protons and electrons usually penetrate into both Earth's (Krivolutsky *et al* 2005) and Titan's (Luna *et al* 2003, Mitchell *et al* 2005) atmospheres causing dissociation of N_2. The synergy among impinging and produced ions and the planetary magnetosphere can be quite complex and a good example of this was recently shown by the Cassini mission to Saturn and Titan. *In situ* measurements of the energetic ion composition showed a Saturn magnetosphere rich in water-group ions and surprisingly depleted of N^+, suggesting little escape of N or N_2 from Titan's atmosphere as would be expected (Krimigis *et al* 2005,

Gombosi and Hansen 2005, Young *et al* 2005). The reason why the N abundance is too low is not clear, one possibility being through some mechanism which inhibits the atmospheric escape. If that is the case, the history of the ions and neutral atoms in their way through the atmosphere must be followed in detail.

Helium ions are easily found in the interplanetary space and have also been detected in Titan's magnetosphere (Krimigis *et al* 2005). High energy He ions, with energies up to 8 MeV have been recently observed in the Earth's polar cusp region when the magnetic field strength is greatly depressed (Chen and Fritz 1999, 2005). As these He ions are likely to come from the solar wind, which has energies typically around 1 keV, some acceleration mechanism, still not understood, must be invoked. In addition to the high energy He ions observed in the Earth's polar cusp region, high energy O^+ ions were also observed, ions which are unlikely to come from the solar wind due to its low charge state. This observation points towards different sources of ions feeding the region where the acceleration mechanism takes place (Chen and Fritz 2005). A full understanding of complex phenomena of this kind is likely to come from a combination of local measurements and Monte Carlo simulations. The latter must be fed by good quality electron and ion ionization and fragmentation data in order to account for the large variety of projectile types and charge states, energies and collision channels which are present. In this work we perform measurements covering an important energy range, from the point of view of collision dynamics, of dissociative collisions of swift He^+ with N_2.

The molecular fragmentation pattern induced by dressed ions is highly dependent on the collision channels and on their efficiency in producing double ionization (Knudsen *et al* 1995, Werner *et al* 1997, Siegmann *et al* 2002, Luna and Montenegro, 2005). In particular, electron loss (stripping) of the projectile is a quite effective collision channel in producing fragmentation. To investigate this behaviour and to compare it with a softer collision mechanism we have carried out absolute measurements of both total projectile electron loss and of partial single and multiple ionization cross sections of He^+ projectiles on N_2, using coincidence and non-coincidence techniques, in the energy range from 0.75 to 3.5 MeV.

2. Experiment

The experimental apparatus has been described in detail in previous publications (Santos *et al* 2001, 2002). In brief, a collimated, monoenergetic He^+ ion beam (with a energy resolution of one part in 200) is delivered by the 4 MV Van de Graaff accelerator of the Catholic University of Rio de Janeiro. The beam is charge analysed by a magnet placed just at the entrance of the gas cell in order to separate the main beam from spurious ones. The two measured emergent charge states, He^+ and He^{2+}, are charge analysed by a second magnet and recorded by two surface barrier detectors nestled in a detection chamber located 4 m downstream. The singly and multiply charged atomic and molecular fragments produced by the primary beam, under single collision conditions, are accelerated by a two-stage electric field and detected by two microchannel plate detectors in a chevron configuration. They provide stop signals to two time-to-amplitude converters started by the signals from the surface barrier detectors. Figure 1 shows time-of-flight spectra of the recoil ions created in the gas cell. The large and constant extraction field ensures that even ions with substantial kinetic energy differences are collected with equal efficiency. The microchannel plate detector also determines the efficiency with which the fragments are recorded. However, special care was taken to obtain detection efficiencies of the multiply charged recoil ions, which were achieved by measuring recoils in coincidence with the single capture of C^{3+} from noble gases (He, Ne, Ar, Kr and Xe) (Santos *et al* 2002).

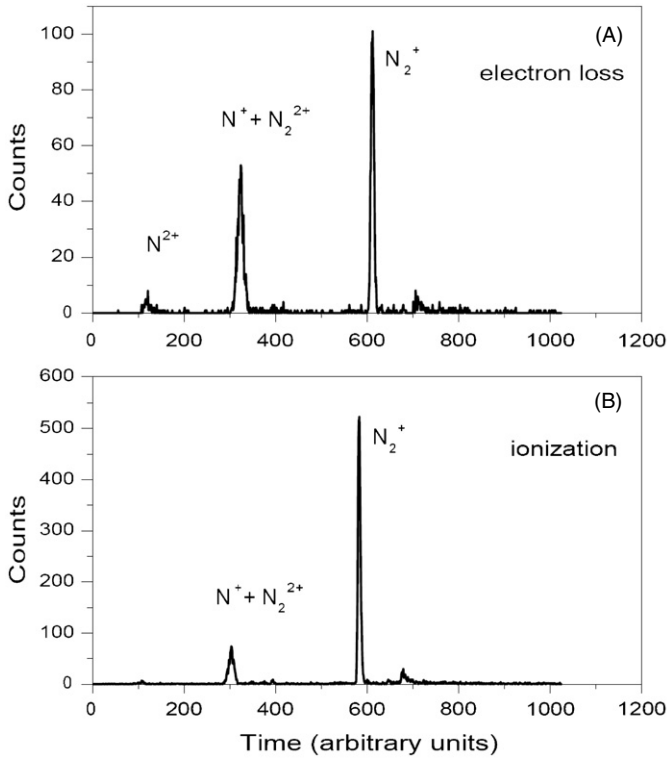

Figure 1. Time-of-flight spectra of N_2 corresponding to the projectile electron loss (A) and direct ionization (B) collision channels for 2.0 MeV He^+ projectiles.

Total absolute projectile electron loss cross sections were obtained by the growth-rate method (see, e.g. Sant'Anna *et al* (1995)). In order to guarantee single-collision conditions, the pressures used, whose absolute values were measured by a capacitive manometer, were always kept below 2 mT. The effective target length is 7.2 cm.

3. Results

The results for single (total loss) and coincidence measurements are listed in table 1. The main sources of uncertainties are due to pressure and background fluctuations (∼2%), impurities in the gas targets due to the gas-admittance system (∼3%), and the effective length of the cell (9–11%).

3.1. Single measurements: projectile electron loss

Figure 2 presents the total measured electron-loss cross section as a function of the projectile velocity, for He^+ impinging in N_2. The present results are in agreement, within experimental errors, with data from Pivovar *et al* (1962) and Dmitriev *et al* (1983). The data from Itoh *et al* (1980) present discrepancies from other results, being systematically below the present results. This behaviour is pointed out by these authors, but the reasons for the observed discrepancies are not clear.

It is interesting to note at this point that the shape and magnitude of the present single projectile electron loss is very similar to previous data obtained for the Ar target (Sant'Anna

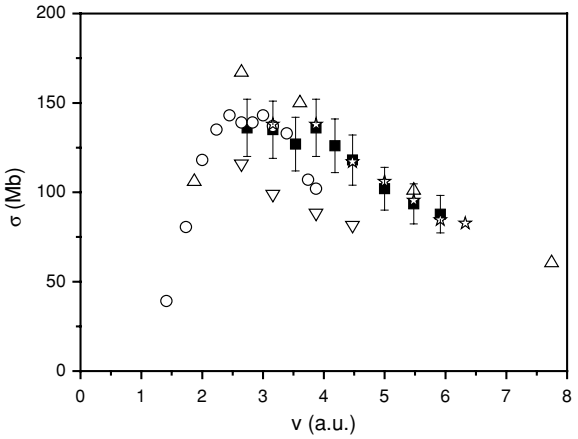

Figure 2. Total electron loss from He^+ projectiles in N_2 as a function of the projectile velocity. (■), this work; (○), Pivovar *et al* (1962); (△), Dmitriev *et al* (1983); (▽), Itoh *et al* (1980). The (☆) represent the electron loss data from He^+ in Ar, from Sant'Anna *et al* (1995), included for the sake of comparison.

Table 1. The cross sections in Mb (10^{-18} cm^2) of total single electron loss, projectile electron loss in coincidence with final target states and direct ionization of N_2 by He^+.

$He^+ + N_2$ cross sections (Mb)							
		Target ionization			Loss with target ionization		
E (MeV)	Total loss	N_2^+	$N_2^{2+} + N^+$	N^{2+}	N_2^+	$N_2^{2+} + N^+$	N^{2+}
0.75	136 ± 16	230 ± 35	75.6 ± 11.5		42.8 ± 6.6	53.6 ± 8.2	
1.00	135 ± 16	213 ± 32	58.5 ± 8.9	2.7 ± 0.5	42.5 ± 6.5	44.3 ± 6.8	5.2 ± 0.9
1.25	127 ± 15	202 ± 30	55.6 ± 8.5	3.5 ± 0.6	45.1 ± 6.9	42.4 ± 6.5	4.4 ± 0.8
1.50	136 ± 16	188 ± 28	48.6 ± 7.5	2.2 ± 0.5	45.9 ± 7.0	38.9 ± 6.0	3.8 ± 0.7
1.75	126 ± 15	172 ± 26	44.2 ± 6.8	2.0 ± 0.4	43.5 ± 6.7	32.9 ± 5.1	2.9 ± 0.6
2.00	118 ± 14	165 ± 25	41.7 ± 6.5	1.3 ± 0.3	40.0 ± 6.2	30.3 ± 4.8	2.5 ± 0.5
2.50	102 ± 12	138 ± 21	32.5 ± 5.1	1.1 ± 0.3	32.6 ± 5.2	21.2 ± 3.5	2.0 ± 0.5
3.00	93.5 ± 11.2	124 ± 19	27.6 ± 4.5	0.82 ± 0.26	27.7 ± 4.5	17.2 ± 2.9	1.3 ± 0.4
3.50	87.7 ± 10.5	112 ± 17	24.9 ± 4.0	0.86 ± 0.26	23.9 ± 3.9	15.0 ± 2.5	1.2 ± 0.3

et al 1995), which are also shown in figure 2. We will return to this feature later, together with the discussion of the coincidence measurements.

3.2. Coincidence measurements: ionization

In this section we discuss the present results for the following reaction channels:

$$He^+ + N_2 \rightarrow He^+ + N_2^+ + e^- \quad (1)$$

$$He^+ + N_2 \rightarrow He^+ + N^+ + N + e^- \quad (2)$$

$$He^+ + N_2 \rightarrow He^+ + N_2^{2+} + 2e^- \quad (3)$$

$$He^+ + N_2 \rightarrow He^+ + N^{2+} + N + 2e^- \quad (4)$$

$$He^+ + N_2 \rightarrow He^+ + N^+ + N^+ + 2e^-. \quad (5)$$

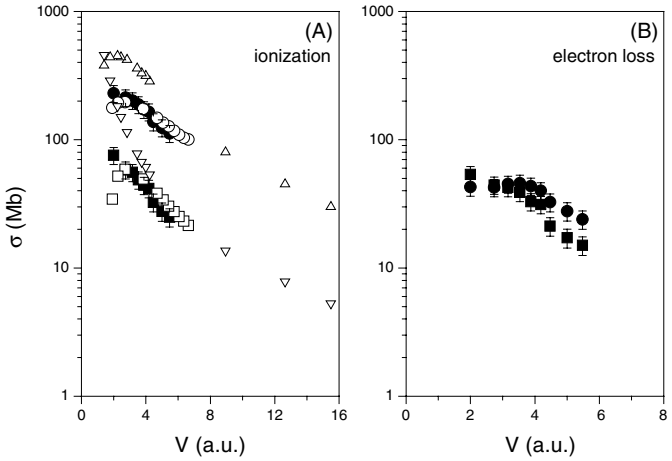

Figure 3. Cross sections for N_2^+ and N^+ production through (A) target ionization and (B) projectile loss channels by He^+, protons and electrons. (A): He^+ projectiles, (●) N_2^+ and (■) N^+, this work; H^+ projectiles, (△) N_2^+ and (▽) N^+, Knudsen *et al* (1995); (☆) N_2^+ and (◇) N^+, Luna *et al* (2003); e^- projectiles, (○) N_2^+ and (□) N^+, Tian and Vidal (1998). (B): He^+ projectiles, (●) N_2^+ and (■) N^+, this work.

Process (1) corresponds to the non-dissociative single target ionization, while process (2) corresponds to the dissociative single target ionization. Process (3) corresponds to non-dissociative double target ionization. Processes (4) and (5) correspond to dissociative double ionization, the latter being accompanied with charge separation. Processes (2) and (3) cannot be distinguished in this experiment because both fragments have the same mass-to-charge ratio (see figure 1).

Figure 3(A) shows our measured cross sections for N_2^+ and N^+ production by He^+ through the ionization channel. These cross sections are compared with those by electrons from Tian and Vidal (1998) and protons from Knudsen *et al* (1995) and Luna *et al* (2003). There is a good agreement between these three singly-charged projectiles in the intermediate-to-high velocity regime, but some discrepancies appear at lower velocities with respect to the proton measurements, mainly for N_2^+ production. Figure 4(A) shows our results for N^{2+} production, also compared with electron- and proton-induced fragmentation. The agreement between electrons, protons and He^+ projectiles for intermediate-to-high velocities is very good and, in this case, no discrepancies are found with respect to protons. The good agreement among these singly-charged projectiles reflects the small orbital radius of the 1s electron of He^+ (approximately 0.25Å) compared with the N_2 bond lengths, which is 1.10 Å for the ground state (Levine 2000), making the He^+ behave essentially as a bare projectile, with charge one, in the process of production of singly- and doubly-charged recoil ions (N_2^+, N^+ and N^{2+}). This behaviour is in agreement with previous measurements by Santos *et al* (2001), of He^+ on noble gases, covering the same velocity range. Indeed, that work shows that even for double and triple ionization of Ar, Kr and Xe, where closer and harder collisions would be expected, which could eventually result in a larger effective charge for He^+, the cross sections for multiple ionization by He^+ and protons are, within the experimental uncertainties, the same. It should be noted that, at low velocities, the electron data present a different behaviour than those for the impact of heavier projectiles, which is due to the threshold for electron impact ionization.

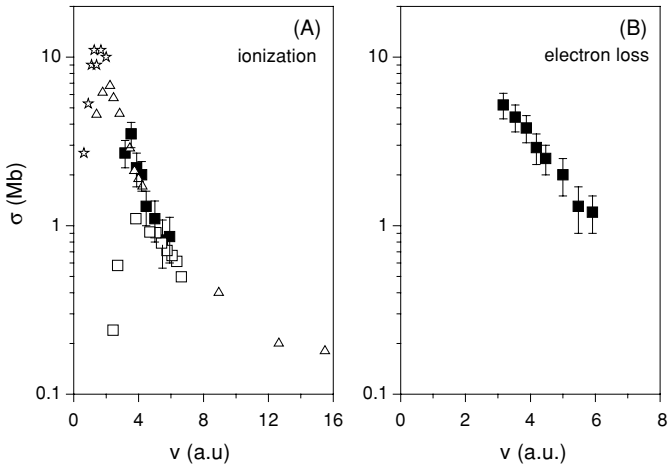

Figure 4. Cross sections for N^{2+} production through (A) target ionization and (B) projectile loss channels by He^+, protons and electrons. Figure 3(A): He^+ projectiles, (■) this work; H^+ projectiles, (△) Knudsen *et al* (1995); (☆) Luna *et al* (2003); e^- projectiles, (□) Tian and Vidal (1998). Figure 3(B): He^+ projectiles, (■) this work.

3.3. Coincidence measurements: electron loss

In this section we discuss the present results for the following reaction channels, all of them involving the ionization of the projectile (electron loss):

$$He^+ + N_2 \rightarrow He^{2+} + N_2^+ + 2e^- \quad (6)$$

$$He^+ + N_2 \rightarrow He^{2+} + N^+ + N + 2e^- \quad (7)$$

$$He^+ + N_2 \rightarrow He^{2+} + N_2^{2+} + 3e^- \quad (8)$$

$$He^+ + N_2 \rightarrow He^{2+} + N^{2+} + N + 3e^- \quad (9)$$

$$He^+ + N_2 \rightarrow He^{2+} + N_2 + e^- \quad (10)$$

$$He^+ + N_2 \rightarrow He^{2+} + N^+ + N^+ + 3e^-. \quad (11)$$

Processes (6) and (7) correspond to single ionization of the target. Processes (8), (9) and (11) correspond to double ionization of the target. These processes can be associated either with the antiscreening process, where the target electrons actively participate as ionizing agents of the projectile, or with a two-centre double ionization, where there is the simultaneous ionization of the projectile and the target electrons by the screened nuclei of the target and projectile, respectively. Processes (7) and (8) cannot be distinguished in the present experiment because they have the same mass-to-charge ratio. Process (10) corresponds to projectile electron loss without target ionization. The main contribution to this process comes from the so-called screening channel, where the target electrons passively screen the target nucleus. Nevertheless, the target excitation part of the antiscreening also contributes to this process, but it is expected to be a small fraction of (5) (Montenegro *et al* 1992). The present experimental set-up cannot detect both fragments from process (11); consequently, this process is not distinguished from process (7).

Figure 3(B) shows our measured cross sections for N_2^+ and N^+ production by He^+ through the electron loss channel. It is clear from the comparison with figure 3(A) that the N_2^+

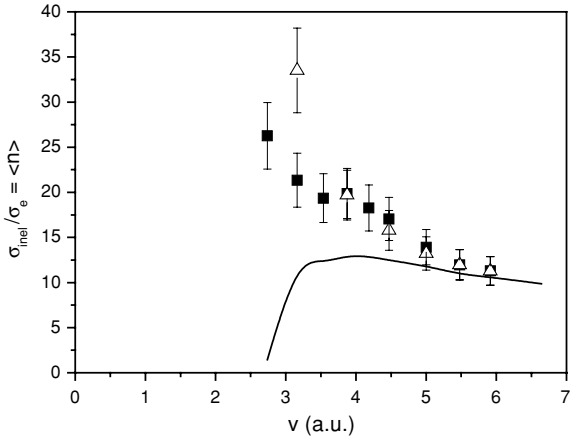

Figure 5. Ratios between $\sigma_{\text{inelastic}}$ and the cross section for electron impact ionization of He^+, σ_e, as a function of the projectile velocity. (■) this work, N_2 target; (△) Sant'Anna *et al* (1995), Ar target. The full line is obtained by making $\sigma_{\text{inelastic}} = \sigma_{\text{anti}}$, with σ_{anti} calculated through the PWBA (see text).

production in this case is strongly inhibited in relation with the ionization channel, while the N^+ production is approximately of the same order for both of them. On the other hand, the production of N^{2+} is slightly enhanced as compared with the ionization channel, as shown in figures 4(A) and (B).

These results can be further analysed with the aid of figure 5, where the ratio between the total inelastic electron loss, $\sigma_{\text{inel}} = \sigma_{N_2^+} + \sigma_{N^+} + \sigma_{N^{2+}}$, and the cross section σ_e for electron impact ionization of He^+ taken from the measurements of Peart *et al* (1969) is shown. For the sake of comparison, similar ratios for Ar $\left(\sigma_{\text{inel}} = \sum_q \sigma_{Ar^{q+}}\right)$ are also shown in figure 5 (Montenegro *et al* 2002). As mentioned before, the simultaneous projectile and target ionization is due to two independent mechanisms: (a) a two-step process in which the projectile is ionized by the screened target while the target is ionized by the screened projectile (loss ionization, LI) and (b) a single, correlated, two-electron process (antiscreening) where the electron–electron interaction between the projectile and target active electrons results in the simultaneous ionization of both. At low velocities, near and below the antiscreening threshold, LI dominates. For velocities above the antiscreening threshold the LI process drops rapidly with the increase of the projectile velocity and the antiscreening dominates the inelastic electron loss (Montenegro *et al* 1994, 2002, Montanari *et al* 2003, Voitkiv 2004). In this region, $\sigma_{\text{inel}} \cong \sigma_{\text{anti}} \cong \langle n\rangle\sigma_e$, where $\langle n\rangle$ is the number of active electrons. Thus, $\sigma_{\text{inel}}/\sigma_e \cong \langle n\rangle$. The ratio $\sigma_{\text{anti}}/\sigma_e$ is shown by the full line in figure 5, with σ_{anti} calculated through the PWBA for He^+ on Ar. It can be seen that the experimental ratio $\sigma_{\text{inel}}/\sigma_e$ for both N_2 and Ar clearly deviates from $\sigma_{\text{anti}}/\sigma_e$ as the projectile velocity decreases towards the antiscreening threshold, indicating that LI becomes progressively important at lower velocities. For $v > 5$ au the antiscreening becomes the dominant mechanism for the simultaneous ionization of the projectile and the target.

The impressive agreement between N_2 and Ar for both the total (figure 2) and the inelastic (figure 5) electron loss cross sections brings an interesting comparison related to the screening contribution. The screening contribution competes with the inelastic one to the total electron loss and comes from events where the target remains in the ground state while the projectile is ionized. The ionization of the projectile is, in this mode, due to the action of the screened

nucleus of the target. Thus, if both total and inelastic cross sections for projectile electron loss in Ar and N_2 are the same, within the experimental errors, the screening cross section is also the same for both targets. This conclusion implies that the Ar screened nuclear charge is as effective as two screened N nucleus to induce the ionization of He^+. This is an unexpected result, due to the large difference between the nuclear charge of Ar compared with that of N, unless the main contribution comes from collisions occurring around the periphery of the target, where the effective charge is near one. Closer collisions are more sensitive to differences in nuclear charge and the present result indicates that they are not important for the stripping of He^+.

As mentioned above, the LI channel is a two-step process involving the projectile ionization through the screening mode together with the target ionization. Because the peripherycal collisions associated with the screening are closer compared to those contributing to ionization, LI involves closer collisions in comparison with ionization. Thus, apart from removing electrons from the non-bonding 1π orbital, LI can be more effective than ionization in removing electrons from 2σ and 3σ bond orbitals of N_2, increasing the probability of breaking the N_2 molecule, as shown in figure 3.

4. Scaling of the fragmentation fraction

The results from Cavalcanti *et al* (2002, 2003) on multiple ionization of noble gases and from Scully *et al* (2006) on fragmentation of water by protons and electrons, indicate that, at high velocities, the multiple ionization and the fragmentation patterns present a very weak dependence on the projectile velocity. This behaviour reflects a post-collisional Auger-like relaxation pattern which follows the process of energy transfer to the system during the collision producing inner-shell vacancies. These results lead us to present here a scaling law based on the *ansatz* that, at high velocities, the fragmentation fraction $f = N^+/(N^+ + N_2{}^+)$ is a function of the energy transfer Q while, at intermediate velocities, it is a function of the momentum transfer Q/v.

The present measurements on ionization and projectile electron loss by He^+ together with previous measurements of electron capture Luna *et al* (2003), ionization by protons (Knudsen *et al* 1995, Luna *et al* 2003) ionization by electrons (Tian and Vidal 1998) and ionization by Ar^{12+} (Tawara *et al* 1986), cover a broad range of projectile velocities and energy transfers—associated with the different collision channels—for fragmentation of N_2. Indeed, for the ionization, electron loss and electron capture channels, the energy transfers are approximately given by $Q_{\rm ion} = I_{\rm t}/R_\infty$, $Q_{\rm loss} = (I_{\rm t} + I_{\rm p})/R_\infty$ and $Q_{\rm cap} = (I_{\rm t} - I_{\rm f})/R_\infty + (v/v_0)^2$, respectively, with R_∞ being the Rydberg constant and v_0 the Bohr velocity. $I_{\rm t}$ is the average ionization energy of N_2, $I_{\rm p}$ is the ionization energy of the active projectile electron and $I_{\rm f}$ is the energy of the final state of the captured electron, respectively. In the following we use $I_{\rm t} = 17.8$ eV, $I_{\rm p} = 54.4$ eV for He^+ projectiles and $I_{\rm f} = 13.6$ eV for proton impact. We found that the relation

$$f(Q, v) = \frac{N^+}{N^+ + N_2^+} = 0.115 \frac{\sqrt{Q}}{1 - \exp\left(-\frac{1}{2}\sqrt{\frac{v}{v_0}}\right)} \tag{12}$$

gives a very good scaling for the fragmentation of N_2, for several projectiles and collision channels, covering a rather large range of projectile velocities. This is shown in figure 6. As mentioned above, this function was built to behave as $f(Q,v) \sim \sqrt{Q}$ at high velocities and as $\sqrt{Q/v}$ at intermediate-to-low velocities.

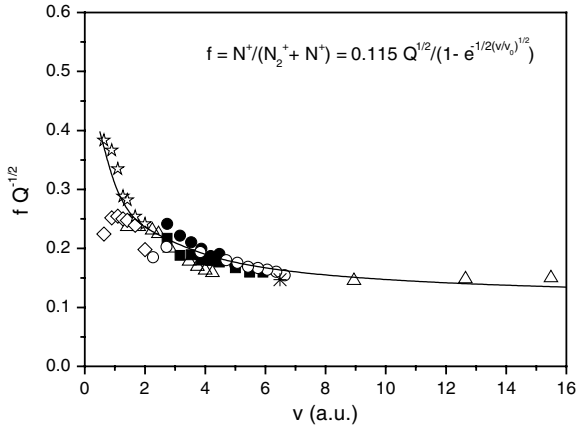

Figure 6. Scaled fragmentation fractions of N_2 for various projectiles and collision channels as a function of projectile velocity. Q is the energy transfer corresponding to each collision channel (see text). (■) ionization by He^+, this work; (●) electron loss by He^+, this work; (△) ionization by protons, Knudsen *et al* (1995); (☆) ionization by protons, Luna *et al* (2003); (◇) ionization by electrons, Tian and Vidal (1998), (∗) ionization by Ar^{12+}, Tawara *et al* (1986). Q and v are plotted in atomic units.

5. Conclusions

Absolute cross sections for total projectile electron loss and target ionization in coincidence with the final charge states of the projectile were measured for 0.75–3.5 MeV He^+ projectiles colliding with N_2 targets. Our results for total projectile electron loss are in good agreement with the majority of the existing measurements. The processes leading to the target ionization contribute with 70 to 45% to the total projectile stripping cross section, decreasing with the projectile energy. For the direct target ionization channel, the present results are very similar to both electron and proton impact data at high velocities, indicating that He^+ behaves essentially as a bare particle with charge equal to 1. It is also found that the fragmentation fractions, f, for singly-charged recoil products, scale quite well as $f(Q,v) \sim \sqrt{Q}$ at high velocities and as $\sqrt{Q/v}$ at intermediate-to-low velocities for all collision channels. This result is useful to estimate fragmentation fractions of N_2 by swift ions with arbitrary charge states and energies, as for example, in simulations of high altitude chemistry following the high particle fluxes impinging on the polar cups, after major solar flares, which present a broad range of particle types and energies (Krivolutsky *et al* 2005).

Acknowledgments

This work is supported in part by the Brazilian agencies CNPq, FAPERJ, CAPES and MCT.

References

Cavalcanti E G, Sigaud G M, Montenegro E C, Sant'Anna M M and Schmidt-Böcking H 2002 *J. Phys. B: At. Mol. Opt. Phys.* **35** 3937

Cavalcanti E G, Sigaud G M, Montenegro E C and Schmidt-Böcking H 2003 *J. Phys. B: At. Mol. Opt. Phys.* **36** 3087

Chen J and Fritz T A 1999 *Adv. Space Res.* **24** 103

Chen J and Fritz T A 2005 *Surv. Geophys.* **26** 71

Dmitriev I S, Vorob`ev N F, Konovalova Zh M, Nikolaev V S and Novozhilova V N 1983 *Sov. Phys.—JETP* **57** 1157

Gombosi T I and Hansen K C 2005 *Science* **307** 1224
Itoh A, Ohnishi K and Furuzawa F 1980 *J. Phys. Soc. Japan* **49** 1513
Knudsen H *et al* 1995 *J. Phys. B: At. Mol. Opt. Phys.* **28** 3569
Krimigis S M *et al* 2005 *Science* **307** 1270
Krivolutsky A, Kuminov A and Vyushkov T 2005 *J. Atm. Sol.-Terr. Phys.* **67** 105
Levine I N 2000 *Quantum Chemistry* 5th edn (Englewood Cliffs, NJ: Prentice-Hall)
Luna H, Michael M, Shah M B, Johnson R E, Latimer C J and McConkey J W 2003 *J. Geophys. Res.* **108** 14–1
Luna H and Montenegro E C 2005 *Phys. Rev. Lett.* **94** 043201
Mitchell D G *et al* 2005 *Science* **308** 989
Montanari C C, Miraglia J E and Arista N R 2003 *Phys. Rev.* A **67** 062702
Montenegro E C, Melo W S, Meyerhof W E and de Pinho A G 1992 *Phys. Rev. Lett.* **69** 3033
Montenegro E C, Meyerhof W E and McGuire J H 1994 *Adv. At. Mol. Opt. Phys.* **34** 249
Montenegro E C, Santos A C F, Melo W S, Sant'Anna M M and Sigaud G M 2002 *Phys. Rev. Lett.* **88** 013201
Peart B, Walton D S and Dolder K T 1969 *J. Phys. B: At. Mol. Phys.* **2** 1347
Pivovar L I, Tubaev V M and Novikov M T 1962 *Sov. Phys.—JETP* **14** 20
Sant'Anna M M, Melo W S, Santos A C F, Sigaud G M and Montenegro E C 1995 *Nucl. Instrum. Methods Phys. Res.* B **99** 46
Santos A C F, Melo W S, Sant'Anna M M, Sigaud G M and Montenegro E C 2001 *Phys. Rev.* A **63** 062717
Santos A C F, Melo W S, Sant'Anna M M, Sigaud G M and Montenegro E C 2002 *Rev. Sci. Instrum.* **73** 2369
Scully S W, Wyer J A, Senthil V, Shah M B and Montenegro E C 2006 *Phys. Rev.* A **73** 040701
Siegmann B, Werner U, Kaliman Z, Roller-Lutz Z, Kabachnick N M and Lutz H O 2002 *Phys. Rev.* A **66** 052701
Tian C and Vidal C R 1998 *J. Phys. B: At. Mol. Opt. Phys.* **31** 5369
Tawara H *et al* 1986 *Phys. Rev.* A **33** 1385
Voitkiv A B 2004 *Phys. Rep.* **392** 191
Werner U, Kabachnik N M, Kondratyev V N and Lutz H O 1997 *Phys. Rev. Lett.* **79** 1662
Young *et al* 2005 *Science* **307** 1262